



Performance Prediction of Magnetless Direct Current Machine using Finite Element Analysis

C. C. Awah

Department of Electrical and Electronic Engineering, Michael Okpara University of Agriculture, Umudike, Nigeria
awahchukwuemeka@gmail.com

Research Article

Abstract

A direct current (DC) electric machine devoid of permanent magnets is developed and analyzed in this paper using finite element analysis (FEA) simulation approach. The investigated machine modules include: flux linkage, electromotive force (EMF), rotor magnetic force, output torque, and core loss. It is revealed that the output characteristics of the investigated machine are closely related to its electric loading and its rotor angular speed; thus, the higher the value of these two parameters, the larger its electromagnetic output performance. For instance, the obtained force magnitudes of the analyzed machine at fixed speed of 500 rpm and varying armature current of 5 A, 10 A, 15 A and 20 A are 31.26 N, 63.18 N, 95.75 N, and 128.97 N, respectively. Similarly, the resultant electromotive force amplitudes of the machine at different rotor speed i.e. 500 rpm, 1000 rpm, 1500 rpm, 2000 rpm, and 2500 rpm are 0.28 mV, 0.56 mV, 0.83 mV, 1.11 mV, and 1.38 mV, respectively. The analyzed machine would be suitable for low speed direct drive applications, owing to its brushless nature.

Copyright © Faculty of Engineering, Ahmadu Bello University, Zaria, Nigeria.

Keywords

Core loss; Direct current; EMF; Flux linkage; Magnet less machine; Torque.

Article History

Received: – April, 2021

Reviewed: – June, 2021

Accepted: – August, 2021

Published: – August, 2021

1. Introduction

Researches toward electric machines that are free of permanent magnets (PMs) are regularly increasing due to the scarcity and exorbitant price of permanent magnets. PM machines are usually susceptible to demagnetization, especially at high working speed and temperature, besides its monopolized market price. Hence, it is pertinent to investigate alternative electrical machine with low-cost materials, which is the overall idea presented in this work.

Significant research on magnet less machines has been carried out due to their potentials which include: cost-usefulness, rotor ruggedness, good field weakening and fault tolerance capabilities, etc. While tremendous investigations are still ongoing with several structural modifications in order to enhance its torque density and power density abilities and possibly efficiency enhancement, as shown in Xu *et al.*, (2016) and Zhou *et al.*, (2020). Moreover, a further study on low-cost DC machine has shown that magnetless DC machine has an additional advantage of high reliability and improved safety over conventional machines, as presented in Lee *et al.*, (2017), for in-wheel direct drive applications. More so, DC magnet-free variable flux reluctance machines and vernier reluctance machines of different structural topologies are attracting more research consideration, due to its intrinsic good qualities such as: broader operating speed coverage, rotor toughness, and good flux-controllability; though, with some disadvantages of low power factor and large loss magnitude (Jia *et al.*, 2016) and Jia *et al.*, (2018).

Shi *et al.*, (2007) proposed a low-cost electric machine which is free of PMs and capable of producing reasonable output torque, though simulated with Personal Simulation Program with Integrated Circuit Emphasis (PSpice) through modeling, which is less accurate when compared to the adopted finite element analysis (FEA) approach in this current work. Although, the FEA consumes a lot of time in calculating the needed results unlike the PSpice and other analytical methods like the magnetic circuit analysis (MCA) procedure which provides fairly accurate results within a very short period by modeling and simplifying the nodal equations, as demonstrated in Yu *et al.*, (2015). Nevertheless, Yu *et al.*, (2015) noted that the investigated machine would have very poor efficiency and limited application when interfaced with three-phase and multi-phase systems, in comparison with other existing machines; in addition to its complicated structural arrangement. However, a more flexible electrical machine in terms of low cost, high magnetic field regulation and improved multi-phasing abilities is developed in Lee *et al.*, (2015) for wind energy systems, with competitive electromagnetic performance compared with permanent magnet flux-reversal machine.

Also, an efficient MATLAB-based software package with high flexibility which is capable of analyzing most electrical machine parameters ranging from its proficiency in predicting the machine's electromotive force, magnetomotive force, to total harmonic distortion calculations is presented in Tommaso *et al.*, (2015); though, the presented simulation software would

require a lot of experience and skill(s) in post-processing of the results for the complete analysis, since it lacks the ability to estimate the winding resistance, number coils, the required quantity of conductor, etc.

The output performance of a given magnetless machine could be improved by using a higher number of poles on the rotor part against that on the stator, Bilgin *et al.*, (2012); in particular, magnetless machines with modular rotor structure seems to produce larger torque than the conventional ones, as stated in Nikam *et al.*, (2012). Luong *et al.*, (2018) proved that wound-field machine having modular stator structure has comparable flux-weakening and fault-tolerant potentials with that of surface-mounted permanent magnet machines. Additionally, the use of modular stator structure in electric machines could enhance its slot packing factor and reduce its resulting copper loss values. More electromagnetic improvement(s) could be realized from such segmented machines when the magnetization sources are hybridized by augmenting the flux contributions from the wound-field windings with a bit of that from permanent magnet sources. However, research has shown that magnetless electric machines are usually characterized with enormous noise, high torque pulsations and consequent large vibrations on the machine compared with other conventional permanent magnet machines (Khan *et al.*, 2017).

Tang *et al.*, (2014) shows that generation of output torque in direct current magnetless machine is dependent on both its flux linkage and inductance variations with the rotor angular positions; these variations would have its peak and least inductance magnitudes at instances when the rotor and stator poles are in aligned and unaligned positions with each other, respectively. Note that the above instances would correspond to the machine's best and least electromagnetic performance points. Zhu *et al.*, (2017) reported that the electromagnetic performance of a given magnetless machine in terms of efficiency and output torque could be enriched significantly by splitting its stator tooth per pole, besides the adequate implementation of the right stator and rotor pole combinations. Zhu *et al.*, (2017) noted that the stator tooth modification would invariably influence the machine's compactness positively and as well reduce its natural high torque ripple weakness; albeit, with higher core loss value when compared with that of conventional machines of similar size and category. The efficacy of splitting the stator tooth and enhancing the machine's performance through excitation hybridization with little PM material is detailed in Farahani *et al.*, (2020) using the following procedures: analytical technique, finite element analysis and laboratory tests.

The analyzed PM-free direct current electrical machine in this present study is depicted in Figure 1. It is worth noting that the presented magnet less machine has no brushes, slip-rings and commutators, and hence would have less maintenance requirement(s) compared to other magnetless machine topologies.

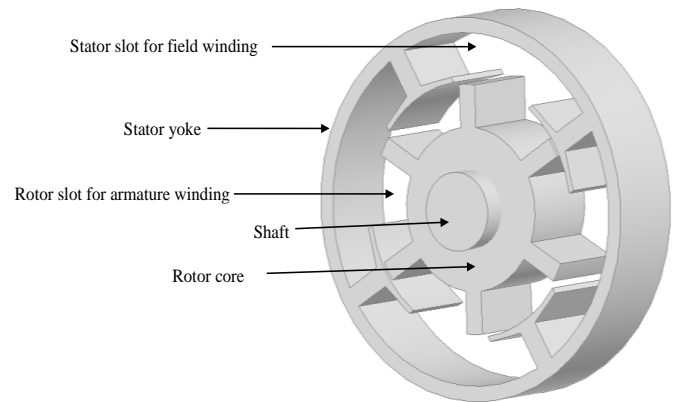


Figure 1. The investigated direct current magnetless machine FEA model.

Essentially, the effectiveness of using the finite element analysis approach to predict electric machine parameters is implemented in this present work which is different from the mathematical modeling approach that is usually based on assumptions, such as uniformly distributed air-gap flux density, etc. Hence, the employed finite element method exhibits high calculation accuracy and reliability. The four sections of this study are Introduction, Methodology, Results and Discussion, and Conclusion.

2. Methodology

The investigated machine is studied using a finite element analysis (FEA) technique. The diameter of the analyzed machine is 90mm while its active stack length is 25mm. The in-built material properties of the used software is assigned to the various machine sections, for instance, the assigned material for the windings is copper while core sections are assigned with steel properties. More so, tiny mesh elements are used to ensure improved result precision. The employed finite element software would automatically calculate the performance characteristics on running the model of Figure 1 and generate the results numerically. Further post-result processing may be required for graphical neatness using Microsoft Excel and MATLAB Plotting Settings. The rotor structure of the investigated machine is made of steel core material and it is identical with that of a typical switched reluctance machine. It should be noted that the excitation sources of the machine is connected on the stator while the rotor is equipped with only the armature windings, hence there is a reduction on the magnetic coupling effects between these two set of windings for enhanced fault-tolerance skill. It is worth mentioning that both the excitation and armature windings are operated with DC sources. More so, there is high tendency for flux regulation flexibility in the developed machine by manipulating the magnitude of the field currents to either enhance or weaken the flux amplitude to suit various purposes. It is also worth noting that individual parametric optimization of the machine geometric variables is employed in this study; thus, an improved machine performance is expected on conducting a global optimization technique (Zhu and Liu 2011) for a given electric machine; possibly with

multi-objectives such as high torque, low ripple, low harmonic distortion, and minimum magnetic force preferences, etc. The mathematical expression of core loss, in electrical machines is given in equation (1).

$$W_c(W/m^3) = k_h B_{max}^2 f k_p + \sum_{\Delta T} \left[\sigma \frac{d^2}{12} \left(\frac{dB}{dt}(t) \right)^2 + k_a \left(\frac{dB}{dt}(t) \right)^{1.5} \right] \Delta T f k_p \quad (1)$$

Where: k_h and k_a are the loss coefficients due to hysteresis and anomalous settings, k_p is the winding packing factor, f is the electrical frequency, T is electric period, B_{max} is the peak air gap flux-density, d is the lamination thickness, and σ is the material conductivity (Wrobel *et al*, 2008).

Similarly, the instantaneous torque, T_i of a given electrical machines is expressed in equation (2).

$$T_i = \frac{e_a i_a + e_b i_b + e_c i_c}{\omega_b} + T_{nl} \quad (2)$$

Where: e_a, e_b, e_c are the phase voltages, $i_a, i_b,$ and i_c are the corresponding supplied phase currents, ω_b is the rotor angular velocity, and T_{nl} is the no-load torque.

This work's feasible combination of the stator and rotor pole numbers is given in equation (3).

$$P_r = 2 \times P_s - 2 \quad (3)$$

Where: P_r and P_s are the rotor and stator pole numbers. Note that P_s should be greater than or equal to 4. The deployed low-silicon steel core material has its magnetic flux density and magnetic field intensity (B-H) data given in Table 1.

The basic finite element analysis (FEA) procedures used in obtaining the presented results in this work are itemized below:

1. Creation and face building of the different model geometric sections, in order to form the complete simulation model.
2. Selection of the desired solution type i.e. the solvers, which could be transient, magneto static, electrostatic, etc. depending on applications; however transient mode is adopted in this current study since the analysis requires both time-varying electric and magnetic fields.
3. Assignment of material properties using the intrinsic values in the software or imported values. All the used material properties in this work are gotten from the in-built software material store.
4. Mesh generation of the different parts using tiny elements for high precision.
5. Creation and addition of the windings: this will depend on the number of phases employed and the preferred excitation conditions such as the voltage expressions, and current or current density levels. The excitation parameter in this work is the current.
6. Creation of the Motion Setup alongside the rotor band and the geometric boundaries. This basically, involves the assignment of rotational or translational parts with the

relevant speed or velocity, respectively. The analyzed machine is a rotary type.

7. Optimization of the model using either the in-built optimization algorithms or application of parametric optimization. Note that parametric optimization is adopted in this work due to time constraint.
8. Simulation of the model geometry and extraction of the numerical FEA results of varying parameters relevant to this specific investigation. Finally, post-processing of the results for enhanced graphical display.

Table 1: B–H Magnetization Data

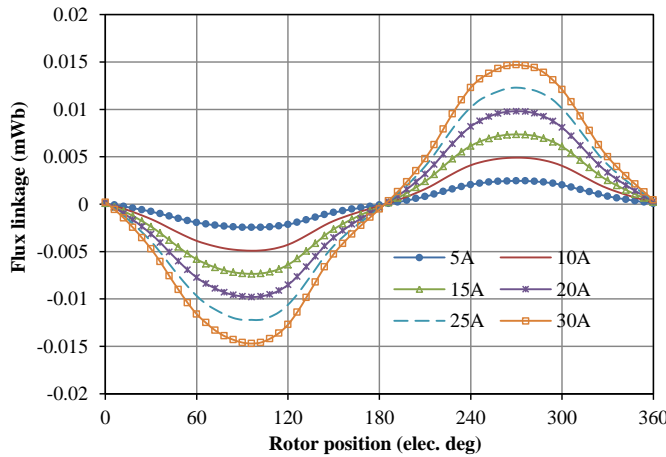
B (T)	H (AT/m)
0	0
9	0.10000000000000001
18	0.20000000000000001
28	0.29999999999999999
37	0.40000000000000002
46	0.5
56	0.59999999999999998
70	0.69999999999999996
88	0.80000000000000004
110	0.90000000000000002
145	1
190	1.10000000000000001
260	1.2
360	1.3
620	1.39999999999999999
1550	1.5
3500	1.60000000000000001
6600	1.7
12000	1.8
20000	1.89999999999999999
33000	2
50000	2.10000000000000001
300000	2.41415926499999999

Source: Electrical Machines and Drives Research Group, the University of Sheffield, UK.

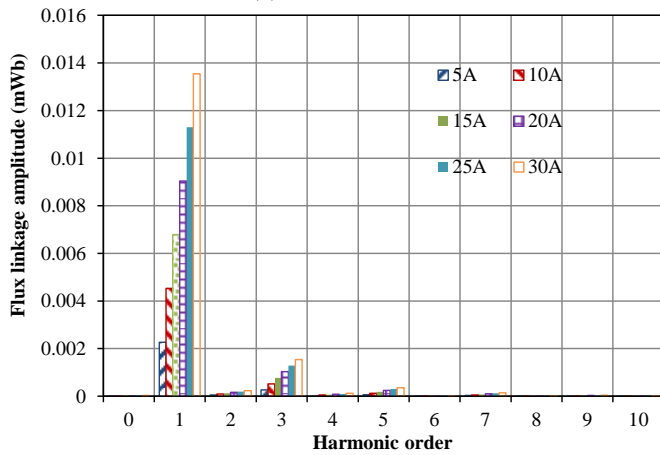
3. Results and Discussion

The predicted flux linkage waveform is depicted in Figure 2. It is observed that the resultant flux linkage waveform is sinusoidal and symmetrical across the simulated rotor positions. This sinusoidal waveform virtue is desired for smooth control of electrical machines. Moreover, the flux linkage variations over the rotor positions are directly proportional to the changes in the input armature current. Larger amount of flux linkage would yield a corresponding larger EMF value and consequently improved overall output torque. The peak value of the flux linkage at 15A is about 0.0074 mWb with a corresponding EMF value of 0.708mV, at operating speed of 500rpm. More so, the variation of induced-electromotive force (EMF) with both the rotor angular positions and armature currents is shown in Figure 3(a). It could be seen that there is a direct proportionality between the resulting EMF and the input currents. Similarly,

the results reveal that the electromagnetic performance of the analyzed machine would also depend on the machine's operating speed as well as its electric loadings, as depicted in Figure 3(c); thus, the larger the speed and electric load of the machine, then, the higher the obtained EMF values and consequently, other output electromagnetic values.



(a) Waveforms

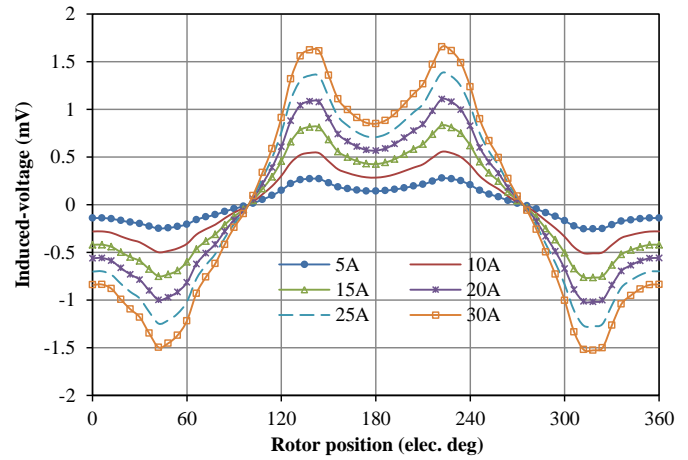


(b) Spectra

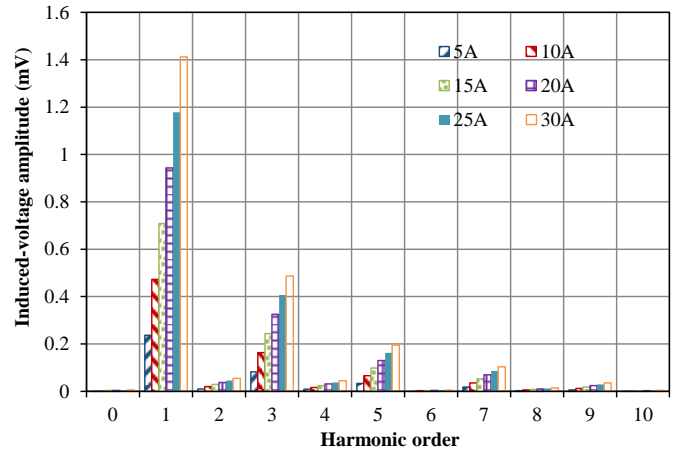
Figure 2. Comparison of flux linkage.

Further, the investigated machine has a lot of voltage harmonics as shown in Figure 3(b), and this will pose some difficulties in its smooth operation with power electronic devices. It is worth noting that the induced-voltage waveforms are non-sinusoidal; thus, this phenomenon would heighten the level of torque ripple in such machine. These noticeable harmonic traits would give rise to increased total harmonic distortion (THD), larger torque ripple and cogging torque in the system, as declared in Shi *et al.* (2014), Sikder *et al.* (2015), and Li *et al.* (2019). Meanwhile, a recent study in Zhao *et al.* (2020) shows that the magnitude of an induced-voltage of a given electric generator is inversely related to its resulting total harmonic distortion, when operated at rated power condition; in other words, larger amplitude of the induced-voltage would yield lower amount of THD, under such situation. It is worth mentioning that a smaller amount of

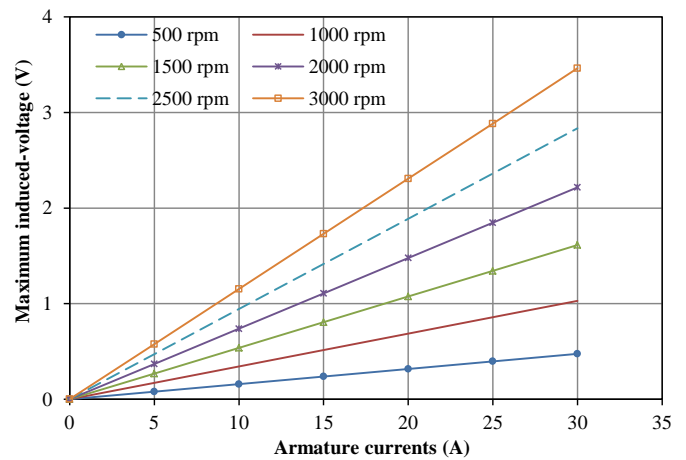
THD could result to a loss reduction in the machine and would possibly give room for enhanced machine performance.



(a) Waveforms



(b) Spectra



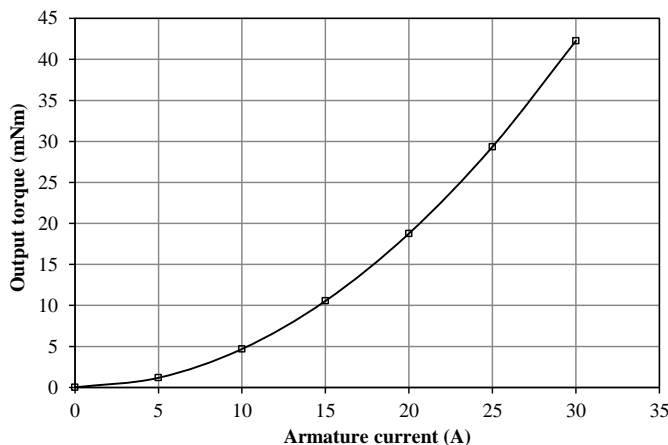
(c) EMF versus speed

Figure 3. Comparison of induced-EMF.

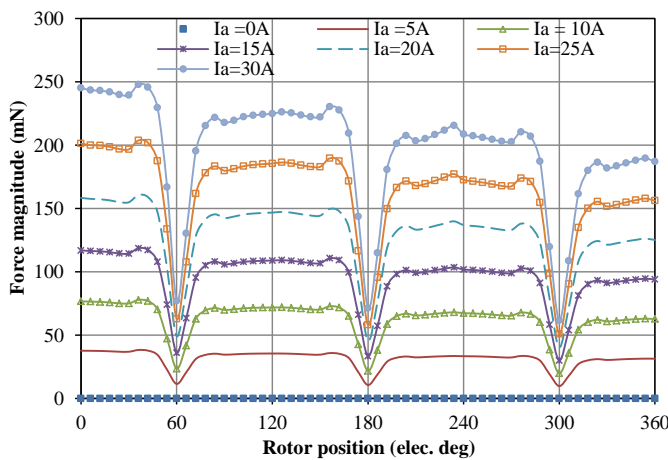
Moreover, the 5th and 7th harmonic contents would imply high cogging torque values and high ripple effect, which is a

demerit, since it will adversely affect the resultant output torque in the system. However, this poor torque defect could be ameliorated by introducing corresponding 5th order current harmonics in the system, through a suitable electric machine control technique, as detailed in Wang *et al*, (2015). The conspicuous 3rd order voltage harmonic component shown in Figure 3(b) is due to the adopted delta winding connection, which would cancel out in a star-connected winding topology, in line with the theoretical concepts. Similarly, the voltage variation with both speed and armature current displayed in Figure 3(c) indicates a direct linear relationship between these variables, i.e. the higher the machine's speed and or input armature current; then, the larger its corresponding voltage, and vice-versa.

Further, Figure 4(a) shows the variation of output torque with the supplied armature current. It could be seen that the resultant torque varies directly proportional to the input armature current. Similarly, the rotor magnetic force results shown in Figure 4(b) show that the amplitude of this force in one electric cycle would be dependent on the amount of injected current and the angular positions of the rotor.



(a) Torque versus armature current

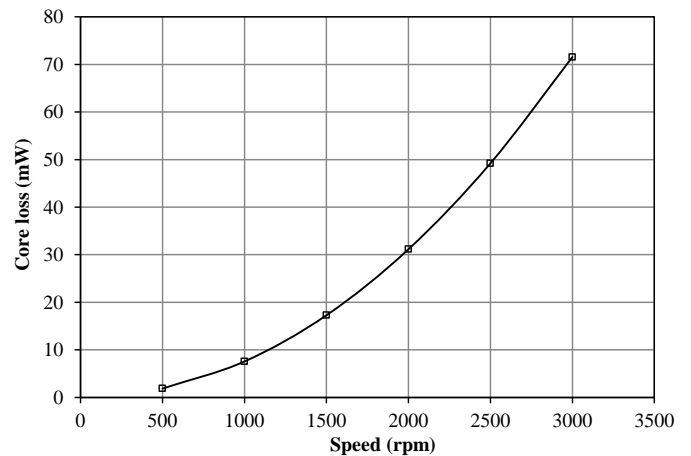


(b) Force versus rotor position

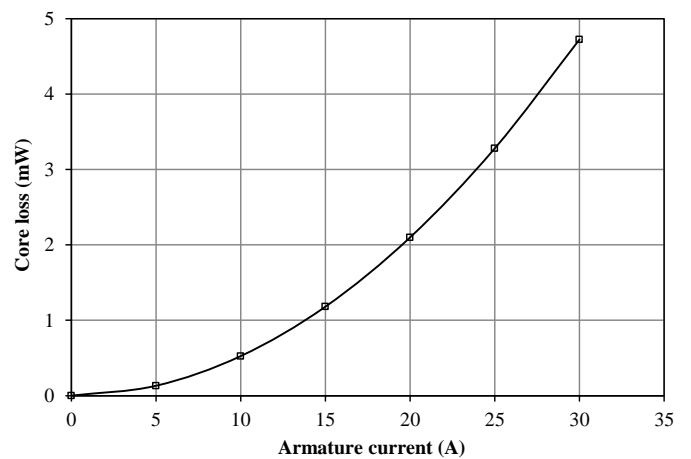
Figure 4. Comparison of output torque and force.

It should be noted that the presence of eccentricities or asymmetry owing to the fabrication tolerance of an electric machine would not only affect the unbalanced magnetic force on the rotor, but would also aggravate its loss profile, as pointed out in Wang *et al*, (2019). Though, radial magnetic force caused by open circuit faults could be reduced in a given electric machine by employing modular structures, as established in Song *et al*, (2018).

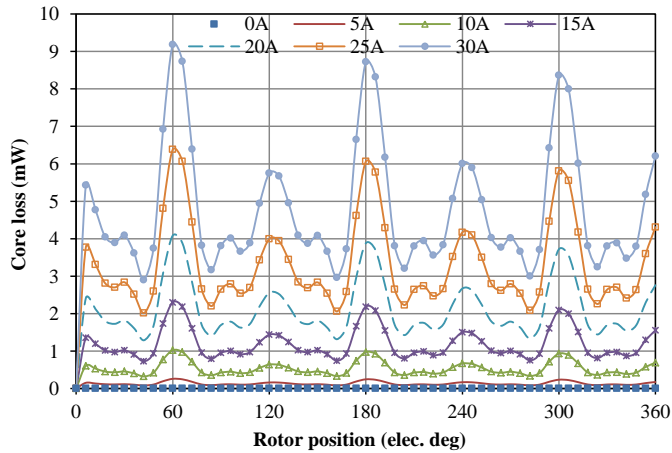
Furthermore, Figures 5 (a) and (b) show the comparison of core loss with rotational speed and armature current, respectively. It is observed that the core loss values have non-linear relationships with both the rotational speed and armature current; moreover, the larger the speed and or armature current magnitude, the higher the resulting core loss value. Hence, there is a need to monitor these parameters' effect to avoid possible saturation of the machine's electromagnetic circuit. In addition, the resultant core loss amplitude of an electric machine is a function of its rotor angular positions, as displayed in Figure 5(c).



(a) Core loss versus speed



(b) Core loss versus armature current



(c) Core loss versus rotor position, 500rpm
Figure 5. Comparison of core loss.

Table 2: FEA predicted loss values at different speeds

Speed (rpm)	Core loss (mW)
500	1.852821021
1000	7.55147583
1500	17.27300349
2000	31.13867713
2500	49.21140498
3000	71.55936572

Table 2: FEA predicted loss values at different current ratings

Armature current (A)	Core loss (mW)
0	0.000701389
5	0.131894672
10	0.525446649
15	1.180956097
20	2.099608457
25	3.280706327
30	4.724586289

The finite element analysis (FEA) predicted loss values at different speed and armature currents are listed in Table 2 and 3 respectively. It is obvious from the tables, that the analyzed machine has trivial amount of core loss under different simulation conditions; which is desirable for improved machine overall performance and efficiency. Moreover, rise in both speed and armature current would yield a proportionate increase in core loss magnitude.

4. Conclusion

The electromagnetic characteristics of a magnetless machine are implemented in this paper with finite element software. The predicted results show the direct relationships between machine's output parameters with its corresponding electric loading and rotor rotational speed. Meanwhile, a non-linear relationship exists between the predicted core loss values and

its matching rotor speeds and supplied currents. Since the developed machine is free of permanent magnets, it would be cheaper to produce compared to permanent magnet machines whose magnetic materials are usually expensive and scarce. Meanwhile, it could have applications in direct drive systems, if prototyped; owing to its ability to operate at low speed with good electromagnetic output performance. Overall, the use of finite element analysis (FEA) in predicting the output performances of a given direct current (DC) electric machine having no permanent magnet is demonstrated in this work.

References

- Bilgin, B., Emadi, A., and Krishnamurthy, M. (2012). Design considerations for switched reluctance machines with a higher number of rotor poles. *IEEE Transactions on Industrial Electronics*, 59(10), pp. 3745–3756.
- Farahani, E.F., Kondelaji, M.A.J., and Mirsalim, M. (2020). A new exterior-rotor multiple teeth switched reluctance motor with embedded permanent magnets for torque enhancement. *IEEE Transactions on Magnetics*, 56(2), pp. 1–5.
- Li, J., Wang, K., Li, F., Zhu, S.S., and Liu, C. (2019). Elimination of even-order harmonics and unipolar leakage flux in consequent-pole PM machines by employing N-S-iron-S-N-iron rotor. *IEEE Transactions on Industrial Electronics*, 66(3), pp. 1736–1747.
- Jia, S., Liang, D., Kong, W., Qu, R., Yu, Z., Li, D., and Kou, P. (2018). A high torque density concentrated winding vernier reluctance machine with DC-biased current. *IEEE Transactions on Magnetics*, 54(11), pp. 1–5.
- Jia, S., Qu, R., Li, J., and Li, D. (2016). Principles of stator DC winding excited vernier reluctance machines. *IEEE Transactions on Energy Conversion*, 31(3), pp. 935–946.
- Khan, F., Sulaiman, E., and Ahmad, M.Z. (2017). A novel wound field flux switching machine with salient pole rotor and nonoverlapping windings. *Turkish Journal of Electrical Engineering and Computer Sciences*, 25(2), pp. 950–964.
- Lee, C.H.T., Chau, K.T., and Cao, L. (2017). Development of reliable gearless motors for electric vehicles. *IEEE Transactions on Magnetics*, 53(11), pp. 1–8.
- Lee, C.H.T., Chau, K.T., and Liu, C. (2015). Design and analysis of a cost-effective magnetless multiphase flux-reversal DC-field machine for wind power generation. *IEEE Transactions on Energy Conversion*, 30(4), pp. 1565–1573.

- Luong, H.T.L., Messine, F., Hénaux, C., Mariani, G.B., Voyer, N., and Mollov, S. (2018). 3D electromagnetic and thermal analysis for an optimized wound rotor synchronous machine. *International Conference on Electrical Machines (ICEM)*, Alexandroupoli, Greece, pp. 455–460, IEEE.
- Nikam, S.P., Rallabandi, V., and Fernandes, B.G. (2012). A high-torque-density permanent-magnet free motor for in-wheel electric vehicle application. *IEEE Transactions on Industry Applications*, 48(6), pp. 2287–2295.
- Shi, C., Qiu, J., and Lin, R. (2007). A novel self-commutating low-speed reluctance motor for direct-drive applications. *IEEE Transactions on Industry Applications*, 43(1), pp. 57–65.
- Shi, J.T., Zhu, Z.Q., Wu, D., and Liu, X. (2014). Comparative study of novel synchronous machines having permanent magnets in stator poles. *International Conference on Electrical Machines (ICEM)*, Berlin, Germany, pp. 429–435, IEEE.
- Sikder, C., Husain, I., and Ouyang, W. (2015). Cogging torque reduction in flux-switching permanent-magnet machines by rotor pole shaping. *IEEE Transactions on Industry Applications*, 51(5), pp. 3609–3619.
- Song, Z., Yu, Y., Chai, F., and Tang, Y. (2018). Radial force and vibration calculation for modular permanent magnet synchronous machine with symmetrical and asymmetrical open-circuit faults. *IEEE Transactions on Magnetics*, 54(11), pp. 1–5.
- Tang, Y., Paulides, J.J.H., and Lomonova, E.A. (2014). Energy conversion in DC excited flux-switching machines. *IEEE Transactions on Magnetics*, 50(11), pp. 1–4.
- Tommaso, A.O.D., Genduso, F., and Miceli, R. (2015). A new software tool for design, optimization, and complete analysis of rotating electrical machines windings. *IEEE Transactions on Magnetics*, 51(4), pp. 1–10.
- Wang, D., Lin, H., Yang, H., Zhang, Y., and Lu, X. (2015). Design and analysis of a variable-flux pole-changing permanent magnet memory machine. *IEEE Transactions on Magnetics*, 51(11), pp. 1–4.
- Wang, M., Tong, C., Song, Z., Liu, J., and Zheng, P. (2019). Performance analysis of an axial magnetic-field-modulated brushless double-rotor machine for hybrid electric vehicles. *IEEE Transactions on Industrial Electronics*, 66(1), pp. 806–817.
- Wrobel, R., and Mellor, P.H. (2008). Design considerations of a direct drive brushless machine with concentrated windings. *IEEE Transactions on Energy Conversion*, 23(1), pp. 1–8.
- Xu, Z., Lee, D.H., and Ahn, J.W. (2016). Design and operation characteristics of a novel switched reluctance motor with a segmental rotor. *IEEE Transactions on Industry Applications*, 52(3), pp. 2564–2572.
- Yu, C., Niu, S., Ho, S.L., and Fu, W.N. (2015). Magnetic circuit analysis for a magnetless double-rotor flux switching motor. *IEEE Transactions on Magnetics*, 51(11), pp. 1–5.
- Zhao, H., Liu, C., Song, Z., Wang, W., and Lubin, T. (2020). A dual-modulator magnetic-g geared machine for tidal-power generation. *IEEE Transactions on Magnetics*, 56(8), pp. 1–7.
- Zhou, X., Zhang, L., and Wu, F. (2020). Operating performance enhancing method for doubly salient electromagnetic machine under light load condition. *IEEE Access*, Vol. 8, pp. 112057–112065.
- Zhu, J., Cheng, K.W.E., Xue, X., and Zou, Y. (2017). Design of a new enhanced torque in-wheel switched reluctance motor with divided teeth for electric vehicles. *IEEE Transactions on Magnetics*, 53(11), pp.1–4.
- Zhu, Z.Q., and Liu, X. (2011). Individual and global optimization of switched flux permanent magnet motors. *International Conference on Electrical Machines and Systems*, Beijing, China, pp. 1–6, IEEE.